

LensingFlow: An Automated Workflow for Gravitational Wave Lensing Analyses

Mick Wright^{1,2}*, Justin Janquart^{3,4}†, Paolo Cremonese⁵, Juno C. L. Chan⁶, Alvin K. Y. Li^{7,8,9}, Otto A. Hannuksela⁸, Rico K. L. Lo⁶, Jose M. Ezquiaga⁶, Daniel Williams¹⁰, Michael Williams¹¹, Gregory Ashton¹², Rhiannon Udall⁹, Anupreeta More^{13,14}, Laura Uronen⁸, Ankur Barsode¹⁵, Eungwang Seo¹⁰, David Keitel⁵, Srashti Goyal¹⁶, Jef Heynen³, Anna Liu⁸

¹ *Institute for Gravitational and Subatomic Physics (GRASP), Department of Physics, Utrecht University, Princetonplein 1, 3584 CC Utrecht, The Netherlands*

² *Nikhef—National Institute for Subatomic Physics, Science Park, 1098 XG Amsterdam, The Netherlands*

³ *Centre for Cosmology, Particle Physics, and Phenomenology—CP3, Université Catholique de Louvain, Chemin du Cyclotron, 2—Box L7.01.05, B-1348 Louvain-la-Nueve, Belgium*

⁴ *Royal Observatory of Belgium, Avenue Circulaire, 3, B-1180 Brussels, Belgium*

⁵ *Departament de Física, Universitat de les Illes Balears, IAC3–IEEC, E-07122 Palma, Spain*

⁶ *Center of Gravity, Niels Bohr Institute, Blegdamsvej 17, 2100 Copenhagen, Denmark*

⁷ *RESCEU, The University of Tokyo, Tokyo, 113-0033, Japan*

⁸ *Department of Physics, The Chinese University of Hong Kong, Shatin, Hong Kong*

⁹ *LIGO Laboratory, California Institute of Technology, Pasadena, California 91125, USA*

¹⁰ *SUPA, School of Physics & Astronomy, University of Glasgow, G12 8QQ Glasgow, Scotland*

¹¹ *Institute of Cosmology and Gravitation, University of Portsmouth, PO1 3FX Portsmouth, United Kingdom*

¹² *Department of Physics, Royal Holloway, University of London*

¹³ *Inter-University Centre for Astronomy and Astrophysics (IUCAA), Post Bag 4, Ganeshkhind, Pune 411 007, India*

¹⁴ *Kavli IPMU (WPI), UTIAS, The University of Tokyo, Kashiwa, Chiba 277-8583, Japan*

¹⁵ *International Centre for Theoretical Sciences, Tata Institute of Fundamental Research, Bangalore 560089, India*

¹⁶ *Max Planck Institute for Gravitational Physics (Albert Einstein Institute)*

29 July 2025

ABSTRACT

In this work, we present LENSINGFLOW. This is an implementation of an automated workflow to search for evidence of gravitational lensing in a large series of gravitational wave events. This workflow conducts searches for evidence in all generally considered lensing regimes. The implementation of this workflow is built atop the ASIMOV automation framework and CBCFLOW metadata management software and the resulting product therefore encompasses both the automated running and status checking of jobs in the workflow as well as the automated production and storage of relevant metadata from these jobs to allow for later reproduction. This workflow encompasses a number of existing lensing pipelines and has been designed to accommodate any additional future pipelines to provide both a current and future basis on which to conduct large scale lensing analyses of gravitational wave signal catalogues. The workflow also implements a prioritisation management system for jobs submitted to the schedulers in common usage in computing clusters ensuring both the completion of the workflow across the entire catalogue of events as well as the priority completion of the most significant candidates. As a first proof-of-concept demonstration, we deploy LENSINGFLOW on a mock data challenge comprising 10 signals in which signatures of each lensing regime are represented. LENSINGFLOW successfully ran and identified the candidates from this data through its automated checks of results from constituent analyses.

1 INTRODUCTION

In the intervening years between the initial detection of gravitational waves (GWs) in 2015 (Abbott et al. 2016) and the publication of the most recent catalogue of events, GWTC-3 (Abbott et al. 2023a), the current ground-based detector network, consisting of the two LIGO detectors in the US (Aasi et al. 2015) and the Virgo detector in Italy (Acernese et al. 2015), has detected ~ 90 GW signals. As sensitivities improve, additional detectors—such as KAGRA (Akutsu et al. 2021)—join the network, and both current and future observing runs are carried out—such as the currently ongoing fourth observing run (O4) which at the time of writing has already reported more than 200 candidate detections (LVK Collaborations 2025)—this number will increase at an accelerating rate (Abbott et al. 2020). This ac-

celeration in detections is expected to improve the current scientific analyses conducted using GWs; such as cosmological parameter estimation (Abbott et al. 2023b), inferring the astrophysical population of merging binaries (Abbott et al. 2023c), constraint and observations (Abbott et al. 2021a) of any potential deviations from general relativity (GR), etc.

To ensure that analyses keep pace with the rate of detections as it rapidly increases, it will be important to allow for significant automation of the deployment of these analyses. Indeed, to maintain the tractability of Bayesian parameter estimation (PE) of incoming GW signals, the automation framework ASIMOV was developed to allow for the large scale deployment of such analyses (Williams et al. 2023). Similarly, the vast numbers of individual analyses each produce an

amount of metadata that allows for the analysis to be open and reproducible. Scaling this requires additional effort to ensure that it is well organised and easily traversable for outsiders. The desire and need to achieve this has led to the development of CBCFlow (Ashton et al. 2024) to standardise and organise metadata from current and future GW analyses.

One area of GW-based research in which the increasing rate of detections will have a particularly sharp impact on the required computational resources is the search for gravitational lensing of GWs. Gravitational lensing occurs when a signal passes close by to a massive object on the path between the source and the observer. The warping of space-time around massive objects that is a prediction of GR affects the propagation of that passing signal. The exact effects vary based on the nature of the object serving as the lens but effects include: the production of multiple copies of the signal, phase shifts, modulations of the amplitude, beating patterns from interference and diffractions, and other distortions (Ohanian 1974; Thorne 1982; Deguchi & Watson 1986; Nakamura 1998; Takahashi & Nakamura 2003). Currently searches for signatures of gravitational lensing have been conducted for those events up to the release of GWTC-3 (Hanuksela et al. 2019; Abbott et al. 2021b, 2024; Janquart et al. 2023b, 2024; Chakraborty & Mukherjee 2025) but have not found confident evidence for detection.

The multiple PE-based analyses on a single GW signal searching for the individual distortions resulting from lensing—such as those proposed in Wright & Hendry (2022); Liu et al. (2023); Janquart et al. (2021b) respectively—would already represent an increase in the number of required analyses to fully study for evidence of signatures of gravitational lensing on that signal on a per-waveform-model basis. However, the first mentioned effect of gravitational lensing—the production of multiple signals—quadratically increases the number of analyses required to investigate the lensing hypothesis as now not only does every individual signal require analyses but the combinations of signals must be analysed—such as through the PE-based approaches proposed in Lo & Magana Hernandez (2023) and Janquart et al. (2021a).

In addition to the significant number of such analyses, one must also consider the computational cost of each individual analysis. Performing PE-based approaches on individual signals is already a taxing challenge, and this is only increased when considering combinations. To mitigate this, there exist already a number of approaches to perform a low latency filtering of multiplets to mitigate the need for the PE-based analyses on every candidate multiplet—see e.g. Haris et al. (2018); Goyal et al. (2021); Ezquiaga et al. (2023); Goyal et al. (2024), and Barsode et al. (2025). Such low latency approaches are much less computationally expensive than the PE-based approaches, but are less accurate. They therefore increase the tractability of the searches, but add to the number of analyses that need to be performed as well as introducing the problem of inter-pipeline communication to the workflow for lensing analyses.

To address these potential roadblocks to performing complete lensing analyses as the number and rate of GW detections increases, we here present LENSINGFLOW (Wright et al. 2025)—an implementation of an automated workflow for lensing analyses. It is built atop the ASIMOV automation framework—to allow the analyses to be deployed easily at scale—and leverages the metadata organisation capabilities of CBCFlow to ensure both that its own output metadata is open and reproducible as well as that prior unlensed analyses may be ingested and used by the lensing analyses efficiently, accurately, and in a standardised fashion. Finally, it implements both filtering and prioritisation of high latency PE analyses based on the recommendations from the lower latency investigations which ensures both the com-

pletion of the entire catalogue of events and multiplets as well as the rapid investigation of the most promising candidates. LENSINGFLOW consequently provides a solid foundation for lensing analyses both of actual detector data as well as large-scale simulation studies.

We provide a proof-of-concept demonstration of LENSINGFLOW by applying it to a mock data challenge (MDC) consisting of 10 GW signals. This set contains at least one representation of each of the lensing regimes for which searches are implemented in addition to unlensed signals.

The rest of this work will be laid out as follows. Section 2 provides a brief overview of the theory of gravitational lensing. Section 3 describes the layout of the workflow. Section 4 provides a detailed description of the MDC and the results from this deployment. Finally, section 5 will summarise the conclusions of the work and provide insight into future plans to further improve the automation of lensing analyses.

2 GRAVITATIONAL LENSING

For a detailed description of gravitational lensing theory, we would refer the reader to literature such as Schneider et al. (1992). We will here present a summary limited to the most relevant topics for this work and define the terminology that will be used through-out this work.

As we have noted in Section 1, gravitational lensing is a consequence of a signal passing by a massive object, meaning that any astrophysical object may be the source of lensing. As might be expected from such a wide array of possible sources, the resulting phenomenology differs significantly across the scales of the objects. Whilst lensing may be structured based on the mass scale of the object, we will here define our structuring of lensing-related terminology based upon how the analyses are implemented. We will first note that there are two broad regimes of lensing—those being where the *geometric optics approximation* is valid, and the effects of lensing may be considered purely in terms of the geometry of the system, and the case where a full *wave optics* treatment is required where effects such as diffraction are playing a noticeable role in the signatures imparted. The domain of the validity is dependent upon a combination of the wavelength of the detected signal and the mass of the lensing object.

In the searches for lensing examined here, we consider the scenario in which the primary effect of lensing is the production of multiple copies of that signal—which we will term *images* throughout the rest of the work. In the regime where the geometric optics approximation is valid, these images each have largely identical frequency evolution but are differentiated by an individual *magnification* of the signal amplitude, a *time delay* with respect to when the original unmodified signal would have arrived, and an overall *phase shift* (Schneider et al. 1992). This means that the observed *strain* for the j^{th} lensed image, $h_j^L(f)$ may be given in terms of the unmodified strain produced by the source, $h(f)$, as (Nakamura & Deguchi 1999)

$$h_j^L(f; \theta, \mu_j, \Delta t_j, n_j) = \sqrt{|\mu_j|} \exp(-2\pi i f \Delta t_j + i \pi n_j) h(f; \theta), \quad (1)$$

where: θ represents the set of parameters of the source binary; μ_j the magnification of the image which itself may be defined in terms of the Jacobian between the lens and source plane co-ordinate systems; Δt_j the time delay for the image resulting from a combination of the geometrical path difference as well as Shapiro delay (Shapiro 1964); and n_j the so-termed *Morse index* which may take one of three

discrete values—0, 0.5, and 1. These values of the index correspond to classification of the image as type I, II, or III respectively.

Where the signals are temporally resolvable as individual images, the magnification and time delay do not cause any changes to the signal morphology. Similarly Type I signals which correspond to the case of no overall phase shift and Type III signals which correspond to the case of a sign flip in phase shift which is completely degenerate with a $\pi/2$ shift in the polarisation angle, also experience no effects on the signal morphology. By contrast, however, Type II images experience an overall de-phasing between the modes of the signal which may lead to a detectable distortion in waveforms that have significant higher order mode (HOM) content (Dai et al. 2017; Ezquiaga et al. 2021; Wang et al. 2021; Janquart et al. 2021b; Vijaykumar et al. 2022).

If for a given detector will one decreases the mass of the lensing object, they will reach the regime in which the time delay between the images is less than the duration of the signal itself. If the lensing mass is still sufficiently high that for this detector the geometric optics approximation is still valid, one will have the case of apparently overlapping signals which can lead to the entire set of images being detected as one event with apparent beating patterns in the combined signal. Given the condition that the geometric optics approximation is still valid, this combined signal can be described as the summation of the j images described in Equation 1.

If we are in the case where the wavelength of the GW signal is comparable to the Schwarzschild radius of the lensing object, then the geometric optics approximation will break down and a full wave optics treatment is required to describe the effects on the signal. In this case, the effects of lensing are entirely frequency-dependent modulations of the amplitude of an apparent signal that may provide insight into the nature of the lensing object itself (Takahashi & Nakamura 2003; Cao et al. 2014; Lai et al. 2018; Christian et al. 2018; Dai et al. 2018; Jung & Shin 2019; Diego et al. 2019; Diego 2020; Pagano et al. 2020; Cheung et al. 2021; Mishra et al. 2021; Yeung et al. 2021; Meena et al. 2022; Wright & Hendry 2022). The exact morphology of the strain is highly dependent on the mass density distribution of the lensing object but a general form is given by (Nakamura & Deguchi 1999; Takahashi & Nakamura 2003)

$$F(w, y) = \frac{w}{2\pi i} \int \exp[-iwT(x, y)] d^2x, \quad (2)$$

where w is a dimensionless representation of the frequencies of the GW, and x and y are dimensionless forms of the image and source positions respectively and the integration is over the image plane. The function T computes the dimensionless time delay for a given image position which will vary on a per-lens-model basis. We note here, for completion, that taking the geometric optics approximation is to assert that only the stationary points of the T function are contribution to the result of the above integral, which will yield the summation of Equation 1 over the j images. These stationary points correspond to the individual images discussed when the approximation is valid and the image type corresponds to the kind of stationary point resulting in that image. We finally note that w is defined such that the geometric optics approximation is valid when $w \gg 1$.

3 ANALYSIS WORKFLOW

We now turn to describe the workflow including some brief descriptions of the constituent lensing pipelines—though we would refer the reader again to the literature for more specific details on each pipeline. These references are summarised in Table 1. During the

Table 1. Constituent pipelines integrated within LENSINGFLOW at the time of writing alongside the paper detailing their methodology and implementation. We note that LENSINGFLOW is constructed to easily allow additional pipelines to be integrated in the future based on the needs of the GW lensing community. N.B. in the case of ATLENSTICS whilst the pipeline implements some of the calculations detailed in the associated methodology paper, it was developed purely for convenient implementation of already existing work in the framework.

Pipeline	Methodology Paper
Multiplet Analyses	
LENSID	Goyal et al. (2021)
PHAZAP	Ezquiaga et al. (2023)
POSTERIOR_OVERLAP	Haris et al. (2018)
ATLENSTICS*	More & More (2022)
GOLUM	Janquart et al. (2021a)
HANABI	Lo & Magana Hernandez (2023)
Single Event Analyses	
GOLUM	Janquart et al. (2021b)
GRAVELAMPS	Wright & Hendry (2022)
	Liu et al. (2023)

following discussions, we will assume that prior analyses have been done that covers the initial detection of the GW event and continues through to standard unlensed PE such as that, that would be produced for a catalogue such as GWTC-3 and that the resulting metadata from these events has been used to construct a CBCFlow library. In this work, we have also restricted the multiplet analyses to operate only on the pairs of events for simplicity—though we note that this restriction is not technical in nature for the automated workflow. Consequently the following discussions may naturally be extended to any set of multiplet. Some work has been done to make extended multiplet analysis available in the package, though further work would be required to bring this to equivalent functionality to pair-wise analyses.

3.1 Identification of Lensed Signals

The most complete means of identifying candidate lensed signals or multiplets is identifying the features from each candidate regime and performing dedicated PE implementing those features—jointly for the multiple signals in the case of multiplet analyses. This allows the computation of a Bayes factor between the lensed and unlensed hypotheses. To calibrate the expectations of values from performing these analyses using each of the dedicated PE models, one could then perform a background analysis over a large number of unlensed injections into similar noise features as has been observed for the data. This would then allow the construction of a distribution of these Bayes factors for the unlensed population from which a false alarm probability (FAP) may be computed to give the statistical significance of the candidate Bayes factor.

For lensing analyses, analysis frameworks to do such dedicated PE based searches have been developed both in the context of joint analysis of multiple signals leading to the GOLUM and HANABI pipelines (Janquart et al. 2021b,a, 2023a; Lo & Magana Hernandez 2023) and in the context of single event analysis in both modelled (Wright & Hendry 2022) and unmodelled (Liu et al. 2023) forms, both of which are implemented in the GRAVELAMPS pipeline (Wright et al. 2021).

Each of these aforementioned analyses implements their respective regime of lensing—and in the case of GRAVELAMPS multiple physical models of lens as well as a phenomenological model—and includes wrapping functionality around the PE framework BILBY (Ashton et al. 2019), as well as the BILBY_PIPE (Romero-Shaw et al. 2020)—and

PARALLEL_BILBY (Smith et al. 2020) in the case of HANABI—high-throughput computing interfaces, meaning that the resulting evidence from these investigations may be easily compared with standard unlensed hypothesis outputs for model selection. In the cases of the GRAVELAMPS analyses and the GOLUM Type II analyses which operate on a single signal basis, this comparison is already considered a final Bayes factor for the hypothesis. In the cases of those analyses that operate on multiple signals, one may additionally fold in population information and estimates of selection effects to further refine the comparison to achieve a final comparative Bayes factor (Lo & Magana Hernandez 2023) under these specific population and model assumptions. Consequently, following the lead of e.g. Abbott et al. (2024) we will term the evidence comparison from these joint PE analyses, the *coherence ratio*.

In prior observing runs of the current detector network searches of these regimes have been carried out (Hannuksela et al. 2019; Abbott et al. 2021b, 2024) so far with no confident detections. Performing these prior investigations has been possible with manual launching of each investigation due to the relatively limited number of currently detected events (and consequently a relatively limited number of pairs). However, even at this current level, as is noted in each of the aforementioned references, the entire set of multiplets needed for a complete lensing analysis would prove to be too computationally intensive to analyse fully given the relatively high computational cost of performing them.

The need to avoid this problem in the prior investigations has motivated the development of a number of higher speed but less complete investigations that are able to serve as filters to limit the number of candidate multiplets that require investigation. In general, these analyses the similarity between different subsets of information generated under the unlensed hypotheses. These will support lensed candidates, however, are also unable to rule out co-incidental overlap of unlensed events maintaining the ultimate need for PE based investigations in these cases. We will now describe briefly each of these analyses.

The most broad of these analyses is that proposed by Haris et al. (2018) implemented in the POSTERIOR_OVERLAP pipeline in which the posteriors obtained from standard unlensed PE analysis may be compared through the computation of a data-driven Bayes factor given by

$$\mathcal{B}_U^L = \int \frac{P(\Theta|d_1) P(\Theta|d_2)}{P(\Theta)} d\Theta, \quad (3)$$

where Θ is a subset of the parameters estimated in unlensed analysis. To improve the efficiency of this statistic, Haris et al. (2018) proposed to also include information about the distributions of time delays expected under the unlensed and lensed hypotheses i.e.

$$\mathcal{R}^{\text{gal}} = \frac{P(\Delta t|\mathcal{H}_{\text{SL}})}{P(\Delta t|\mathcal{H}_{\text{UL}})}. \quad (4)$$

More & More (2022) then refined this proposition further to include the remaining effective lensing parameters—the relative magnification and Morse phase shift—to compute the statistic

$$\mathcal{M}^{\text{gal}} = \frac{P(\Delta t, \mu_r, \Delta\psi|\mathcal{H}_{\text{SL}})}{P(\Delta t, \mu_r, \Delta\psi|\mathcal{H}_{\text{UL}})}. \quad (5)$$

These may be computed from extensive catalogues of lensed and unlensed simulations to build the distributions. Using such catalogues, the ATLENTICS pipeline was built as a thin wrapper for the production of these statistics from the posterior samples from unlensed PE investigation. The inclusion of simulations for the production of lensed catalogues, however, does mean that these statistics are only valid under the assumptions used to generate the populations used to create them.

Moving from the complete set of the posteriors, Ezquiaga et al. (2023)—implemented in the PHAZAP pipeline—proposed to perform an analysis of specifically the phase posterior distributions obtained after post-processing the samples to establish a common reference frame. Under the assumption that the posteriors on these detected phases are sufficiently Gaussian, one may quantify the consistency between the posteriors through a distance given by

$$D_{12} = \sqrt{\Delta\theta^T (C_1 + C_2)^{-1} \Delta\theta}, \quad (6)$$

where $\Delta\theta$ is the difference between the parameters for each individual event and the C_i terms indicate the covariances. Computing this quantity over the set of possible orderings and the possible phase differences and maximising the choice from the former and minimising from the latter gives a metric by which to assess pairs. This may be matched with a statistic to measure how well constrained the parameters are to yield an overall ranking of candidates to assess which ones would warrant further analysis with the PE-based analyses.

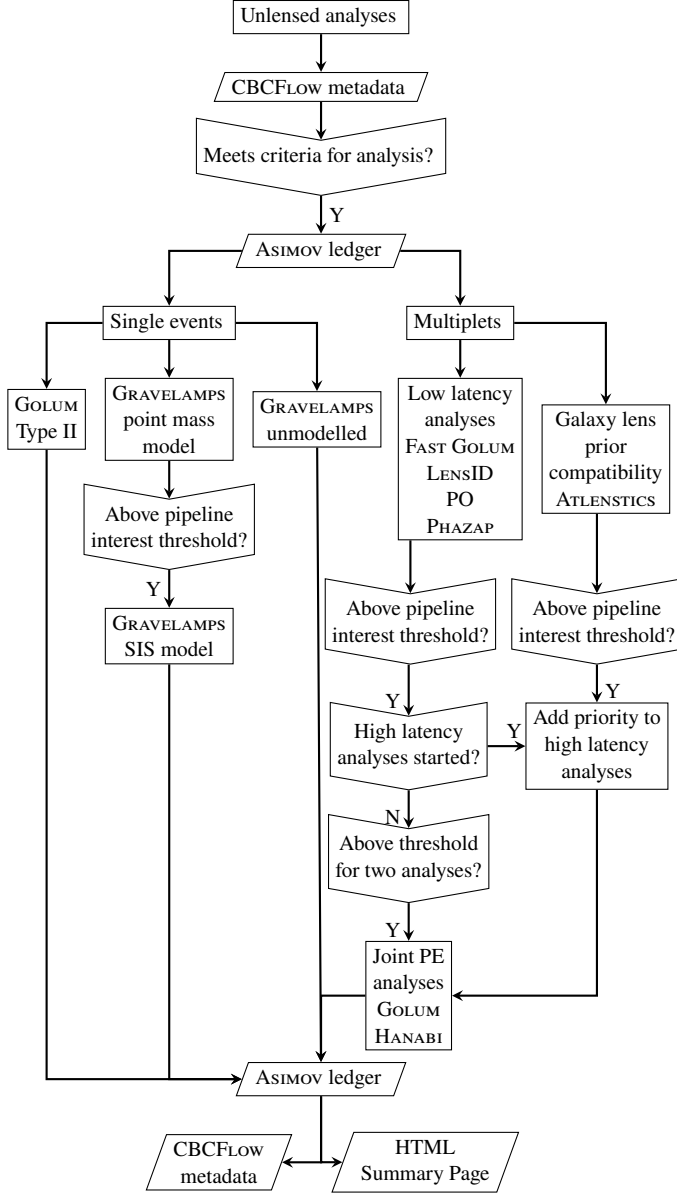
Each of the previous analyses has required the production of full unlensed PE-based analyses in order to assess whether or not a given pair would appear to be consistent with the lensing hypothesis introducing a significant latency between the detection of a GW event and the ability to perform the aforementioned analyses. To circumvent this Goyal et al. (2021) proposed, and implemented in the LENSID pipeline, to use some of the first pieces of information produced in the GW analysis chain—time-frequency maps, also known as Q-transforms, which may be produced directly from incoming data and localization skymaps which are produced rapidly using BAYESTAR (Singer & Price 2016) to identify candidates. They do this by using both of these aforementioned pieces of information as inputs to a machine-learning classifier which combines both intrinsic and extrinsic parameter information encoded in these inputs to identify potential candidates.

3.2 Automated Workflow

We now describe in detail the construction of the automated workflow and the necessary implementations for deploying it in the manner described. A summary of the workflow is provided in Figure 1. We note that to prepare for deployment in the automated workflow, each pipeline was updated to include the necessary implementation of the PIPELINE class (Williams 2025) that makes it usable by the ASIMOV framework (Williams et al. 2023). Each pipeline was then able to produce a standard template of their respective configuration file for which ASIMOV is then able to fill with run-specific information.

The initial stage of work for the production of lensing analyses under the automated workflow is gathering the requisite CBCFlow metadata files into a library of events to be analysed (Ashton et al. 2024). Under general deployment conditions lensing analyses may be considered as part of a larger chain of analyses from initial detection through to unlensed PE, each of which may contribute to a large CBCFlow library containing both GW events as well as transient noise features, so-called “glitches”. The first step implemented is a means to filter events through a selection criteria for lensing analyses. For this work, the selection criteria are that the event is determined to most likely be a binary black hole merger and that the event has been detected by search pipelines, such as GSTLAL (Messick et al. 2017; Sachdev et al. 2019; Cannon et al. 2021; Tsukada et al. 2023) or PyCBC (Biwer et al. 2019; Allen et al. 2012; Allen 2005; Nitz et al. 2017; Dal Canton et al. 2014), that the false alarm rate (FAR) is less than 1 per year. Events passing these criteria are transferred to an individual sub-library for the lensing analyses.

Figure 1. Flowchart summarising the automated workflow implemented by LENSINGFLOW including both the multiplet and single event analyses. We note that the latter stages noting the output to CBCFlow happen repeatedly throughout the process of the deployment of the analyses such that the meta-data is always reflective of the current state of analyses. We also note that whilst the status of the event is always checked after each analysis for interest in the event/pair for that pipeline, the status recorded in the ledger, and ultimately, the outputs, we show this step only for those cases where that check has knock on effects in the deployment of other analyses.



Once the library of metadata is constructed, the next preparatory step is using the information contained within to build an ASIMOV ledger which serves as the central hub for that framework to automate the deployment and monitoring of the analyses of the events and consequent pairs. For pipelines, such as CBCFlow, that are compatible with ASIMOV, this is achieved through a standard APPLICATOR class implemented within the ASIMOV codebase (Williams 2025). Whilst this existed already for CBCFlow and would successfully gather the information needed to produce unlensed analyses, modifications were needed to gather additional information from those unlensed

analyses for the purposes of lensing analyses. These modifications are made available in ASIMOV directly in releases beginning with the 0.6 series.

With the events applied to the ledger, the analysis configurations must be set up for both those analyses that use only that single event as well as those analyses that cover multiplets of events. These are applied using a YAML configuration file that describes essential properties of each analysis. The LENSINGFLOW package produces this file automatically when applying new events and it will generate all necessary individual analyses, as well as both the pairs formed by the newly applied events and those from the new events with those events that are already in the ledger whilst avoiding duplication through the redundant other ordering of each pair—specifically by ensuring that all multiplet-based analyses are done in a time-of-detection ordering and that relevant information about the unlensed analysis configurations and results are retrieved from relevant files linked in the CBCFlow metadata.

The ASIMOV monitor will then use the information given from both the event application as well as the analyses’ configurations to build and submit the requested jobs for the HTCONDOR scheduler (Litzkow et al. 1988) widely used on the cluster computing facilities necessary to facilitate high volume analysis of GW signal data. It will begin with the low latency analyses for multiplets—in this work this consists of LENSID, POSTERIOR_OVERLAP, PHAZAP, and GOLUM operating a conditional pair-wise PE approach—and the check for compatibility with expectations for galaxy lensing using ATLENSTICS, as well as the individual event analysis consisting of the GOLUM Type II PE analysis, and the GRAVELAMPS modelled and unmodelled PE. Upon the completion of each pipeline, the results are automatically analysed to determine if the support for lensing from each pipeline is above a user-defined threshold for that pipeline which warrants additional investigations.

Should a pipeline from the low latency multiplet analyses yield an above-threshold candidate, ASIMOV will wait for additional information before proceeding with any follow-up steps. If a second pipeline concurs, ASIMOV will then start the joint PE analysis pipelines GOLUM and HANABI. Additional low latency pipelines that concur with the two sufficient for starting the high latency analyses will provide additional relative priority in the HTCONDOR scheduler for analyses of this multiplet. Conversely, should enough low latency pipelines indicate a lack of support for lensing such that the starting of the higher latency analyses is no longer possible based on the remaining pipelines, ASIMOV will automatically discard the PE analyses whilst retaining the remaining low latency analyses for the record. We note here that the ATLENSTICS consistency evaluation is not used for the purposes of determining whether the PE-based analyses are started and is instead only used for the purposes of prioritisation. This is to prevent the possibility of prior belief overriding support from the data in regions that are unexpected whilst still rewarding those multiplets that are within expectations.

For the other branches of analyses, only the isolated point mass model analyses causes another analysis to be directly started by ASIMOV in the case when it reports that the analysis has found an above-threshold candidate. In this case, ASIMOV will deploy an additional lens model—the singular isothermal sphere (Binney & Tremaine 1989)—for investigation. This model, whilst not necessarily the most reflective of objects on the physical mass scale that results in single event behaviour, is useful in the context of looking at an extended object vs a more point-like object. For the remaining branches, as well as for any triggered analyses, when they conclude, the same exercise is undertaken with the results analysed to compare to a threshold. In this case, this is simply recorded in the ledger with no direct effects

but does indicate that the event or multiplet should undergo further manual investigations such as those in e.g. [Janquart et al. \(2023b\)](#).

During the entire process, as modifications are made to the ASIMOV ledger, these are also fed back to the CBCFlow metadata through a standard COLLECTOR class implemented within ASIMOV ([Williams 2025](#)). This ensures that these files are kept up-to-date with a current state of analyses. Again, modifications were made here to properly transfer back information from the lensing analyses discussed in this work and are made available in ASIMOV beginning with the 0.6 series. Additionally, the LENSINGFlow package provides automated production of an HTML page to monitor the current state of each analysis in the ledger and provides lists of those jobs that have passed the thresholds for interest and those jobs that have encountered technical difficulties causing them to get stuck, allowing an at-a-glance status update for lensing analyses.

4 EXAMPLE DEPLOYMENT

To provide an initial proof-of-concept deployment of the LENSINGFlow, it was applied to a MDC comprising 16 GW signals that were injected into simulated Gaussian noise drawn from the expected noise power spectral density (PSD) for the currently ongoing fourth observing run ([Collaboration 2022](#)). The parameters from these signals were drawn from a POWERLAW+PEAK merger population model—the parameters of which were themselves drawn from the posterior samples fitting this model to the population of observed binaries from GWTC-3 in [Abbott et al. \(2023c\)](#). Data was generated for the span of ~ 1 month and assuming no detector down-time in a network consisting of the two LIGO detectors and the Virgo detector. Generated systems were then also randomly assigned lensing effects. The signals were produced using the IMRPHENOMXPHM waveform approximant ([Pratten et al. 2021](#)).

Analysis was performed to mirror the detection and catalogue unlensed PE stages for these signals. Of the total number of injected signals, 10 were found by the GSTLAL detection pipeline and were thus subjected to PE analysis and made available to the LENSINGFlow for analysis using CBCFlow metadata files generated from the unlensed analysis results. A summary of the events is provided in Table 2.

We will now briefly summarise the results from those analyses that are able to start downstream analyses based on their results. Beginning with the pair-wise analyses the PHAZAP pipeline identified 6 pairs to be passed to high latency, the POSTERIOR_OVERLAP pipeline identified 3, the LENSID passed 4, and the GOLUM pipeline operating in a conditional approach also identified 6 pairs. A summary of these pairs is provided in Table 3. From the 7 unique pairs identified from these analyses, 6 are above threshold in two or more pipelines and would be passed to the joint PE analyses—which include those that result from the three combinations from the triplet 08a-08b-09x and the pair 10ae-10af which were the injected lensed cases noted in Table 2. All other pairs not listed were discarded. This phase would therefore narrow the total number of pairs that would require analysis from 45 to 6, a $\sim 85\%$ decline in computational burden.

Turning to the isolated point mass analysis, GRAVELAMPS identified both the events MS220508a and MS220526y as worthy of additional investigation—corresponding to the injections with single image lensing applied. That the isolated point mass investigation was able to identify both the modelled and unmodelled events may indicate that a further optimisation that could be made to decrease computational burden would be to analyse events with only this model as a first step. However, further investigations would need to

Table 2. Summary of the detected events used in the MDC to which the LENSINGFlow was applied as a proof-of-concept demonstration. Shown are the name of the event, the individual source frame masses of the primary and secondary, apparent luminosity distance to the system, and the kind(s) of lensing, if any, applied to the event. We note that for Multiplet images (M), the image type is noted. PMS refers to point mass singlet and US to unmodelled singlet respectively. Superscripts identify events belonging to the same lensed system.

Event	Primary Mass (M_{\odot})	Secondary Mass (M_{\odot})	Apparent Luminosity Distance (Mpc)	Lensing Applied
MS220425h	35.5	33.9	5435.0	None
MS220505y	21.2	19.2	1581.8	None
MS220508a ¹	70.1	38.8	2858.2	Type I M + PMS
MS220508b ¹	70.1	38.8	3366.5	Type II M
MS220509x ¹	70.1	38.8	5960.8	Type II M
MS220510af ²	166.9	117.0	9250.3	Type I M
MS220510ae ²	166.9	117.0	10066.8	Type II M
MS220514y	77.8	57.1	7324.3	None
MS220523d	10.2	9.3	1935.2	None
MS220526y	56.1	53.9	3579.4	US

Table 3. Summary of the pairs identified by the low latency pair-wise analyses and which analyses found them.

Pair	FAST GOLUM	LENSID	PHAZAP	POSTERIOR OVERLAP
MS220508a & MS220508b	Y	Y	Y	Y
MS220508a & MS220509x	Y	Y	Y	Y
MS220508b & MS220509x	Y	N	Y	N
MS220510ae & MS220510af	Y	Y	Y	Y
MS220425h & MS220510af	N	N	Y	N
MS220425h & MS220510ae	Y	N	Y	N
MS220510ae & MS220514y	Y	Y	N	N

be carried out for comparative analysis between signals generated from the modelled and unmodelled approaches.

Whilst the remainder of the analyses do not directly contribute to any of the LENSINGFlow functionality directly, we note for completeness that in terms of the automated thresholds which causes LENSINGFlow to note in the metadata that an event/pair requires further investigation—the Type II strong lensing analysis flagged the events MS220508a and MS220425h, and the joint PE analyses flagged all 4 pairs from the lensed events as worthy of additional scrutiny.

From this we may see that the automated operation of the pipelines is able to successfully filter to those candidates that have lensing signatures and start PE based analyses, allowing the continued computational burden reduction that each of these pipelines offer. Aside from the initial input of the CBCFlow metadata files, the operation of these investigations required no manual intervention. In a scaled deployment this would significantly free-up analyst time to devote to specific follow-ups or other investigations allowing more detailed lensing investigations over the course of e.g. an observing run.

5 CONCLUSION

In the coming years, as additional GW detectors come online and the sensitivities of the detectors continues to improve, both the number

and rate of GW detections will continue to rise. It is, therefore, imperative that robust infrastructure is in place to automate currently manually performed analyses. Otherwise, the workload will eventually exceed what can be manually handled in a reasonable amount of time. The need for such automation is particularly strongly felt in analyses for GW lensing in which multiplets of events must be analysed, significantly increasing the workload as compared to non-lensed single event analyses. Additionally, lensing pipelines represent a relatively intricate workflow compared to standard chains of analyses, or sets of non-interdependent analyses which are common in GW analyses, marking a more unique use case for the steps towards automated analysis taken in the community with the development of tools such as CBCFlow (Ashton et al. 2024) and ASIMOV (Williams et al. 2023).

To address these needs of the GW lensing community, in this work we have presented LENSINGFLOW—an automated workflow for lensing analyses using at its base a series of customised modifications to the two aforementioned frameworks as well as custom functionality encoded in a PYTHON package, that we make available freely alongside this work (Wright et al. 2025). This framework provides the means to perform analyses both of individual GW events as well as the pairwise combinations necessary for a full examination of the lensing hypothesis across the different regimes. Currently the framework includes a number of flagship lensing analysis pipelines, but the framework is flexible and able to accommodate additional pipelines to ensure that the needs of the community may continue to be met by it in the future. For example, work has already started for LENSINGFLOW to handle inclusions in CBCFlow metadata files from candidates for searches from sub-threshold searches for faint additional lensed images not included in the original GWTC selections, though those pipelines (McIsaac et al. 2020; Li et al. 2023b,a) have not been fully integrated into the workflow yet.

We demonstrate an initial proof-of-concept deployment on an MDC comprising a set of 10 events including examples of each of the regimes of lensing that analyses consider, under the automated passing criteria, the workflow correctly both generated the more in-depth analyses for the lensed events as well as identifying them for further scrutiny as well as reducing the workload of the most computationally intensive investigations of multiple events by $\sim 85\%$. The automated in-fill of information also prevents the development of inconsistencies between the multiple analyses of the same event/multiplet, ensuring that comparisons between the analyses are always apples-to-apples whilst minimising the human effort required to achieve these needs, which in a realistic deployment would free analyst time for further investigations of any high priority candidates, and other scientific work.

ACKNOWLEDGEMENTS

The authors are grateful to Tomasz Baka for careful review of the paper. The authors are grateful for computational resources provided by the LIGO Laboratory and supported by National Science Foundation Grants PHY-0757058 and PHY-0823459. MW is supported by the research programme of the Netherlands Organisation for Scientific Research (NWO). PC and DK were supported by the Universitat de les Illes Balears (UIB); the Spanish Agencia Estatal de Investigación grants CNS2022-135440, PID2022-138626NB-I00, RED2024-153978-E, RED2024-153735-E, funded by MICIU/AEI/10.13039/501100011033, the European Union NextGenerationEU/PRTR, and the ERDF/EU; and the Comunitat Autònoma de les Illes Balears through the Conselleria d'Educació i Universi-

tats with funds from the European Union–NextGenerationEU/PRTR-C17.I1 (SINCO2022/6719) and from the European Union–European Regional Development Fund (ERDF) (SINCO2022/18146). ES is supported by grants from the College of Science and Engineering at the University of Glasgow. LEU is supported by the Hong Kong PhD Fellowship Scheme (HKPFS) from the Hong Kong Research Grants Council (RGC). OAH and LEU acknowledge support by grants from the Research Grants Council of Hong Kong (Project No. CUHK 14304622, 14307923, and 14307724), the start-up grant from the Chinese University of Hong Kong, and the Direct Grant for Research from the Research Committee of The Chinese University of Hong Kong. JCLC, JME, and RKLL are supported by VILLUM FONDEN (grant no. 53101 and 37766). The Center of Gravity is a Center of Excellence funded by the Danish National Research Foundation under grant No. 184. The Tycho supercomputer hosted at the SCIENCE HPC center at the University of Copenhagen was used for supporting this work. JME is also supported by the European Union's Horizon 2020 research and innovation program under the Marie Skłodowska-Curie grant agreement No. 847523 INTERACTIONS.

REFERENCES

- Aasi, J., et al. 2015, *Class. Quant. Grav.*, 32, 074001, doi: [10.1088/0264-9381/32/7/074001](https://doi.org/10.1088/0264-9381/32/7/074001)
- Abbott, B. P., Abbott, R., Abbott, T. D., et al. 2016, *Phys. Rev. Lett.*, 116, 061102, doi: [10.1103/PhysRevLett.116.061102](https://doi.org/10.1103/PhysRevLett.116.061102)
- . 2020, *Living Reviews in Relativity*, 23, doi: [10.1007/s41114-020-00026-9](https://doi.org/10.1007/s41114-020-00026-9)
- Abbott, R., Abe, H., Acernese, F., et al. 2021a, Tests of General Relativity with GWTC-3. <https://arxiv.org/abs/2112.06861>
- Abbott, R., et al. 2021b, *Astrophys. J.*, 923, 14, doi: [10.3847/1538-4357/ac23db](https://doi.org/10.3847/1538-4357/ac23db)
- Abbott, R., Abbott, T., Acernese, F., et al. 2023a, *Physical Review X*, 13, doi: [10.1103/physrevx.13.041039](https://doi.org/10.1103/physrevx.13.041039)
- Abbott, R., Abe, H., Acernese, F., et al. 2023b, *The Astrophysical Journal*, 949, 76, doi: [10.3847/1538-4357/ac74bb](https://doi.org/10.3847/1538-4357/ac74bb)
- Abbott, R., Abbott, T. D., Acernese, F., et al. 2023c, *Phys. Rev. X*, 13, 011048, doi: [10.1103/PhysRevX.13.011048](https://doi.org/10.1103/PhysRevX.13.011048)
- Abbott, R., et al. 2024, *Astrophys. J.*, 970, 191, doi: [10.3847/1538-4357/ad3e83](https://doi.org/10.3847/1538-4357/ad3e83)
- Acernese, F., et al. 2015, *Class. Quant. Grav.*, 32, 024001, doi: [10.1088/0264-9381/32/2/024001](https://doi.org/10.1088/0264-9381/32/2/024001)
- Akutsu, T., et al. 2021, *PTEP*, 2021, 05A101, doi: [10.1093/ptep/ptaa125](https://doi.org/10.1093/ptep/ptaa125)
- Allen, B. 2005, *Phys. Rev. D*, 71, 062001, doi: [10.1103/PhysRevD.71.062001](https://doi.org/10.1103/PhysRevD.71.062001)
- Allen, B., Anderson, W. G., Brady, P. R., Brown, D. A., & Creighton, J. D. E. 2012, *Phys. Rev. D*, 85, 122006, doi: [10.1103/PhysRevD.85.122006](https://doi.org/10.1103/PhysRevD.85.122006)
- Ashton, G., et al. 2019, *Astrophys. J. Suppl.*, 241, 27, doi: [10.3847/1538-4365/ab06fc](https://doi.org/10.3847/1538-4365/ab06fc)
- . 2024, CBCFlow. <https://cbc.docs.ligo.org/projects/cbcflow/index.html>
- Barsode, A., Goyal, S., & Ajith, P. 2025, *Astrophys. J.*, 980, 258, doi: [10.3847/1538-4357/adae10](https://doi.org/10.3847/1538-4357/adae10)
- Binney, J., & Tremaine, S. 1989, *Galactic dynamics*, doi: [10.1515/9781400828722](https://doi.org/10.1515/9781400828722)
- Biwer, C. M., Capano, C. D., De, S., et al. 2019, *Publ. Astron. Soc. Pac.*, 131, 024503, doi: [10.1088/1538-3873/aaef0b](https://doi.org/10.1088/1538-3873/aaef0b)
- Cannon, K., Caudill, S., Chan, C., et al. 2021, *SoftwareX*, 14, 100680, doi: <https://doi.org/10.1016/j.softx.2021.100680>
- Cao, Z., Li, L.-F., & Wang, Y. 2014, *Phys. Rev. D*, 90, 062003, doi: [10.1103/PhysRevD.90.062003](https://doi.org/10.1103/PhysRevD.90.062003)
- Chakraborty, A., & Mukherjee, S. 2025. <https://arxiv.org/abs/2503.16281>
- Cheung, M. H. Y., Gais, J., Hannuksela, O. A., & Li, T. G. F. 2021, *Mon. Not. Roy. Astron. Soc.*, 503, 3326, doi: [10.1093/mnras/stab579](https://doi.org/10.1093/mnras/stab579)

- Christian, P., Vitale, S., & Loeb, A. 2018, *Phys. Rev. D*, 98, 103022, doi: [10.1103/PhysRevD.98.103022](https://doi.org/10.1103/PhysRevD.98.103022)
- Collaboration, L.-V.-K. 2022, Noise Curves for use in simulations pre-O4, Tech. rep. <https://dcc.ligo.org/LIGO-T2200043/public>
- Dai, L., Li, S.-S., Zackay, B., Mao, S., & Lu, Y. 2018, *Phys. Rev. D*, 98, 104029, doi: [10.1103/PhysRevD.98.104029](https://doi.org/10.1103/PhysRevD.98.104029)
- Dai, L., Venumadhav, T., & Sigurdson, K. 2017, *Phys. Rev. D*, 95, 044011, doi: [10.1103/PhysRevD.95.044011](https://doi.org/10.1103/PhysRevD.95.044011)
- Dal Canton, T., et al. 2014, *Phys. Rev. D*, 90, 082004, doi: [10.1103/PhysRevD.90.082004](https://doi.org/10.1103/PhysRevD.90.082004)
- Deguchi, S., & Watson, W. D. 1986, *Phys. Rev. D*, 34, 1708, doi: [10.1103/PhysRevD.34.1708](https://doi.org/10.1103/PhysRevD.34.1708)
- Diego, J., Hannuksela, O., Kelly, P., et al. 2019, *Astron. Astrophys.*, 627, A130, doi: [10.1051/0004-6361/201935490](https://doi.org/10.1051/0004-6361/201935490)
- Diego, J. M. 2020, *Phys. Rev. D*, 101, 123512, doi: [10.1103/PhysRevD.101.123512](https://doi.org/10.1103/PhysRevD.101.123512)
- Ezquiaga, J. M., Holz, D. E., Hu, W., Lagos, M., & Wald, R. M. 2021, *Phys. Rev. D*, 103, 6, doi: [10.1103/PhysRevD.103.064047](https://doi.org/10.1103/PhysRevD.103.064047)
- Ezquiaga, J. M., Hu, W., & Lo, R. K. L. 2023, *Physical Review D*, 108, doi: [10.1103/physrevd.108.103520](https://doi.org/10.1103/physrevd.108.103520)
- Goyal, S., D., H., Kapadia, S. J., & Ajith, P. 2021, *Physical Review D*, 104, doi: [10.1103/physrevd.104.124057](https://doi.org/10.1103/physrevd.104.124057)
- Goyal, S., Kapadia, S. J., Cudell, J.-R., Li, A. K. Y., & Chan, J. C. L. 2024, *Phys. Rev. D*, 109, 023028, doi: [10.1103/PhysRevD.109.023028](https://doi.org/10.1103/PhysRevD.109.023028)
- Hannuksela, O. A., Haris, K., Ng, K. K. Y., et al. 2019, *Astrophys. J. Lett.*, 874, L2, doi: [10.3847/2041-8213/ab0c0f](https://doi.org/10.3847/2041-8213/ab0c0f)
- Haris, K., Mehta, A. K., Kumar, S., Venumadhav, T., & Ajith, P. 2018, Identifying strongly lensed gravitational wave signals from binary black hole mergers. <https://arxiv.org/abs/1807.07062>
- Janquart, J., Hannuksela, O. A., K., H., & Van Den Broeck, C. 2021a, *Mon. Not. Roy. Astron. Soc.*, doi: [10.1093/mnras/stab1991](https://doi.org/10.1093/mnras/stab1991)
- Janquart, J., Haris, K., Hannuksela, O. A., & Van Den Broeck, C. 2023a, *Mon. Not. Roy. Astron. Soc.*, 526, 3088, doi: [10.1093/mnras/stad2838](https://doi.org/10.1093/mnras/stad2838)
- Janquart, J., Seo, E., Hannuksela, O. A., Li, T. G. F., & Broeck, C. V. D. 2021b, *Astrophys. J. Lett.*, 923, L1, doi: [10.3847/2041-8213/ac3bcf](https://doi.org/10.3847/2041-8213/ac3bcf)
- Janquart, J., Wright, M., Goyal, S., et al. 2023b, *Mon. Not. Roy. Astron. Soc.*, 526, 3832, doi: [10.1093/mnras/stad2909](https://doi.org/10.1093/mnras/stad2909)
- Janquart, J., et al. 2024, doi: [10.1093/mnras/staf049](https://doi.org/10.1093/mnras/staf049)
- Jung, S., & Shin, C. S. 2019, *Phys. Rev. Lett.*, 122, 041103, doi: [10.1103/PhysRevLett.122.041103](https://doi.org/10.1103/PhysRevLett.122.041103)
- Lai, K.-H., Hannuksela, O. A., Herrera-Martín, A., et al. 2018, *Phys. Rev. D*, 98, 083005, doi: [10.1103/PhysRevD.98.083005](https://doi.org/10.1103/PhysRevD.98.083005)
- Li, A. K. Y., Chan, J. C. L., Fong, H., et al. 2023a, <https://arxiv.org/abs/2311.06416>
- Li, A. K. Y., Lo, R. K. L., Sachdev, S., et al. 2023b, *Phys. Rev. D*, 107, 123014, doi: [10.1103/PhysRevD.107.123014](https://doi.org/10.1103/PhysRevD.107.123014)
- Litzkow, M., Livny, M., & Mutka, M. 1988, in *Proceedings of the 8th International Conference of Distributed Computing Systems*
- Liu, A., Wong, I. C. F., Leong, S. H. W., et al. 2023, *Mon. Not. Roy. Astron. Soc.*, 525, 4149, doi: [10.1093/mnras/stad1302](https://doi.org/10.1093/mnras/stad1302)
- Lo, R. K. L., & Magana Hernandez, I. 2023, *Phys. Rev. D*, 107, 123015, doi: [10.1103/PhysRevD.107.123015](https://doi.org/10.1103/PhysRevD.107.123015)
- LVK Collaborations. 2025, GraceDB. <https://gracedb.ligo.org/superevents/public/04/>
- McIsaac, C., Keitel, D., Collett, T., et al. 2020, *Phys. Rev. D*, 102, 084031, doi: [10.1103/PhysRevD.102.084031](https://doi.org/10.1103/PhysRevD.102.084031)
- Meena, A. K., Mishra, A., More, A., Bose, S., & Bagla, J. S. 2022, *Mon. Not. Roy. Astron. Soc.*, 517, 872, doi: [10.1093/mnras/stac2721](https://doi.org/10.1093/mnras/stac2721)
- Messick, C., et al. 2017, *Phys. Rev. D*, 95, 042001, doi: [10.1103/PhysRevD.95.042001](https://doi.org/10.1103/PhysRevD.95.042001)
- Mishra, A., Meena, A. K., More, A., Bose, S., & Bagla, J. S. 2021, *MNRAS*, 508, 4869, doi: [10.1093/mnras/stab2875](https://doi.org/10.1093/mnras/stab2875)
- More, A., & More, S. 2022, *Monthly Notices of the Royal Astronomical Society*, 515, 1044–1051, doi: [10.1093/mnras/stac1704](https://doi.org/10.1093/mnras/stac1704)
- Nakamura, T. T. 1998, *Phys. Rev. Lett.*, 80, 1138, doi: [10.1103/PhysRevLett.80.1138](https://doi.org/10.1103/PhysRevLett.80.1138)
- Nakamura, T. T., & Deguchi, S. 1999, *Prog. Theor. Phys. Suppl.*, 133, 137, doi: [10.1143/ptps.133.137](https://doi.org/10.1143/ptps.133.137)
- Nitz, A. H., Dent, T., Dal Canton, T., Fairhurst, S., & Brown, D. A. 2017, *Astrophys. J.*, 849, 118, doi: [10.3847/1538-4357/aa8f50](https://doi.org/10.3847/1538-4357/aa8f50)
- Ohanian, H. 1974, *Int. J. Theor. Phys.*, 9, 425, doi: [10.1007/BF01810927](https://doi.org/10.1007/BF01810927)
- Pagano, G., Hannuksela, O. A., & Li, T. G. F. 2020, *Astron. Astrophys.*, 643, A167, doi: [10.1051/0004-6361/202038730](https://doi.org/10.1051/0004-6361/202038730)
- Pratten, G., et al. 2021, *Phys. Rev. D*, 103, 104056, doi: [10.1103/PhysRevD.103.104056](https://doi.org/10.1103/PhysRevD.103.104056)
- Romero-Shaw, I. M., et al. 2020, *Mon. Not. Roy. Astron. Soc.*, 499, 3295, doi: [10.1093/mnras/staa2850](https://doi.org/10.1093/mnras/staa2850)
- Sachdev, S., et al. 2019, <https://arxiv.org/abs/1901.08580>
- Schneider, P., Ehlers, J., & Falco, E. E. 1992, *Gravitational Lenses, Astronomy and Astrophysics Library* (Springer), doi: [10.1007/978-3-662-03758-4](https://doi.org/10.1007/978-3-662-03758-4)
- Shapiro, I. I. 1964, *Phys. Rev. Lett.*, 13, 789, doi: [10.1103/PhysRevLett.13.789](https://doi.org/10.1103/PhysRevLett.13.789)
- Singer, L. P., & Price, L. R. 2016, *Phys. Rev. D*, 93, 024013, doi: [10.1103/PhysRevD.93.024013](https://doi.org/10.1103/PhysRevD.93.024013)
- Smith, R. J. E., Ashton, G., Vajpeyi, A., & Talbot, C. 2020, *Mon. Not. Roy. Astron. Soc.*, 498, 4492, doi: [10.1093/mnras/staa2483](https://doi.org/10.1093/mnras/staa2483)
- Takahashi, R., & Nakamura, T. 2003, *Astrophys. J.*, 595, 1039, doi: [10.1086/377430](https://doi.org/10.1086/377430)
- Thorne, K. 1982, in *Les Houches Summer School on Gravitational Radiation*, 1–57
- Tsukada, L., et al. 2023, *Phys. Rev. D*, 108, 043004, doi: [10.1103/PhysRevD.108.043004](https://doi.org/10.1103/PhysRevD.108.043004)
- Vijaykumar, A., Mehta, A. K., & Ganguly, A. 2022, <https://arxiv.org/abs/2202.06334>
- Wang, Y., Lo, R. K. L., Li, A. K. Y., & Chen, Y. 2021, *Phys. Rev. D*, 103, 104055, doi: [10.1103/PhysRevD.103.104055](https://doi.org/10.1103/PhysRevD.103.104055)
- Williams, D. 2025, ASIMOV documentation. <https://asimov.docs.ligo.org/asimov/master/index.html>
- Williams, D., Veitch, J., Chiofalo, M. L., et al. 2023, *Journal of Open Source Software*, 8, 4170, doi: [10.21105/joss.04170](https://doi.org/10.21105/joss.04170)
- Wright, M., & Hendry, M. 2022, *The Astrophysical Journal*, 935, 68, doi: [10.3847/1538-4357/ac7ec2](https://doi.org/10.3847/1538-4357/ac7ec2)
- Wright, M., Janquart, J., & Cremonese, P. 2025, LENSINGFLOW. <https://git.ligo.org/lensingflow/lensingflow>
- Wright, M., Liu, A., Seo, E., Wong, I. C. F., & Janquart, J. 2021, GRAVELAMPS. <https://git.ligo.org/mick.wright/Gravelamps>
- Yeung, S. M. C., Cheung, M. H. Y., Gais, J. A. J., Hannuksela, O. A., & Li, T. G. F. 2021, <https://arxiv.org/abs/2112.07635>